DOI: 10.1002/ejic.201000245

Chain-Type Lithium Rare-Earth Nitridosilicates – $Li_5Ln_5Si_4N_{12}$ with Ln = La, Ce

Saskia Lupart,[a] Martin Zeuner,[a] Sandro Pagano,[a] and Wolfgang Schnick*[a]

Keywords: Solid-state structures / Lithium / Nitridosilicates / Silicon

The quaternary lithium rare-earth nitridosilicates $Li_5Ln_5Si_4N_{12}$ with Ln = La, Ce were synthesized at moderate temperatures below 900 °C in closed tantalum ampoules employing liquid lithium as a flux. Thereby, nitridosilicate substructures with a low degree of condensation were obtained. The air and moisture sensitive title compounds are the first representatives of quaternary lithium rare-earth nitridosilicates and crystallize in space group $P\bar{4}b2$ [$Li_5La_5Si_4N_{12}$: a = 1104.28(16), c = 557.30(11) pm, Z = 2, R_1 = 0.0498, 873 data, 56 parameters; $Li_5Ce_5Si_4N_{12}$: a = 1097.78(16), c = 551.43(11) pm, Z = 2, R_1 = 0.0334, 748 data, 56 parameters]. The nitridosilicate substructure consists of infinite non-branched *zweier* single-chains of vertex sharing SiN_4 tetrahedra running parallel to [001]. The chains exhibit a stretching factor f_S = 0.981 for La and 0.977 for Ce, respectively. The two crystallographically independent Li^+ sites are each coordinated by four nitrogen atoms. Lattice energy calculations (MAPLE) and EDX measurements confirmed the electrostatic bonding interactions and the chemical compositions. For the La containing compound ^{7}Li solid-state MAS NMR investigations are reported.

Introduction

Due to their remarkable properties (e.g. luminescence or lithium ion conductivity) nitridosilicates have become materials of broad academic and industrial interest.[1,2] In this context, doping of alkaline earth nitridosilicates (e.g. $M_2Si_5N_8$, M = Ca, Sr, Ba) with Eu^{2+} or Ce^{3+} lead to highly efficient host lattices for luminescent materials in phosphor-converted (pc)-LEDs.[2–6] Formally, nitridosilicates can be derived from oxosilicates by substituting N for O. Owing to the extended structural possibilities of nitrogen compared to oxygen, nitridosilicates feature a more variable degree of condensation and realize topologically new building blocks. For instance, fourfold coordinated $N^{[4]}$ has been observed in $BaYbSi_4N_7$ which exhibits a "star-shaped" $[N^{[4]}(SiN_3)_4]$ unit, where nitrogen adopts ammonium character.[7] Moreover, neighboring SiN_4 tetrahedra can share corners and even common edges.[8,9] However, most of the nitridosilicates characterized so far contain highly condensed frameworks which is probably due to the employment of high-temperature syntheses (>1300 °C).[10–12] Hence, only two chain-type nitridosilicates were obtained so far. Recently, $M_5Si_3N_9$ with M = La, Ce, Pr[13,14] has been described which exhibits zipper-like chains of vertex sharing SiN_4 tetrahedra due to additional Q^1-type SiN_4 units[15] which are attached to every second tetrahedron of the chain. Quite recently, the mixed valence-type Eu_2SiN_3 has been synthesized by employment of a lithium flux technique at quite low temperatures. This nitridosilicate comprises non-branched *zweier* chains of vertex sharing SiN_4 tetrahedra with a maximum stretching factor f_S = 1.0.[16,17] The use of molten sodium as flux agent for the synthesis of nitridosilicates was introduced by DiSalvo et al. in the case of $Ba_5Si_2N_6$.[18] An analogous synthetic approach resulted in structural characterization of a series of nitridosilicates, e.g. $MSiN_2$ (M = Ca, Sr, Ba),[19] though silicon and nitrogen are only sparingly soluble in liquid sodium.

Therefore, the use of lithium melts affords several advantages for the synthesis of nitridosilicates compared to sodium. Due to the broad spectrum of applications of lithium in radiochemistry the reactivity of liquid lithium with other elements has been well examined.[20–22] It has been shown that both nitrogen and silicon are soluble to a comparable extend in liquid lithium, and moreover, a variety of metals can be solved at moderate temperatures in lithium-rich systems as well.[21] Consequently, the use of lithium melts seemed to be a promising approach for the synthesis of novel nitridosilicates. Recently, we have been able to synthesize a number of quaternary lithium alkaline earth nitridosilicates with varying degrees of condensation employing closed tantalum ampoules.[23] The degree of condensation of the SiN_4 substructures could be directed by the pressure inside the ampoules. Within this context, the structural elucidation of a group-like silicate, namely $Li_4Ca_3Si_2N_6$, with "bow tie" $[Si_2N_6]^{10-}$ units has been accomplished. Furthermore, hitherto unknown intermediates like double-chain nitridosilicates ($LiCa_3Si_2N_5$) could be synthesized using this synthetic approach.[23]

[a] Ludwig-Maximilians-Universität München, Department Chemie, Lehrstuhl für Anorganische Festkörperchemie
Butenandtstraße 5-13, 81377 München, Germany
Fax: +49-89-2180-77440
E-mail: wolfgang.schnick@uni-muenchen.de

Supporting information for this article is available on the WWW under http://dx.doi.org/10.1002/ejic.201000245.

In this contribution we present the first quaternary lithium rare-earth nitridosilicates, namely $Li_5Ln_5Si_4N_{12}$ with Ln = La, Ce. Hence, the liquid lithium approach has been successfully extended to rare-earth materials, forming nonbranched *zweier* single-chain nitridosilicates in closed tantalum ampoules at moderate temperatures.

Results and Discussion

Synthetical Approach

The nitridosilicates $Li_5Ln_5Si_4N_{12}$ (Ln = La, Ce) were obtained by employment of two different synthesis routes. Both routes start from silicon diimide [$Si(NH)_2$] and the corresponding rare-earth chlorides $LnCl_3$ (Ln = La, Ce). Single crystals (cf. Figure 1) of the title compounds could best be obtained by adding lithium as flux to the reaction mixture. Thereby, the amount of excessive lithium remaining in the sample cannot easily be controlled, because contamination occurs due to a certain amount of lithium adhering to the tantalum tube. Therefore, a second synthetic approach utilising LiN_3 as the only lithium source was developed, leading predominately to microcrystalline bulk samples of the title compounds. In contrast to recently reported lithium nitridosilicates ($Li_4Ca_3Si_2N_6$, $Li_2Sr_4Si_4N_8O$ or $LiCa_3Si_2N_5$)[23] no crystalline product was obtained when using Li_3N as the only lithium source. Interestingly, a given nitrogen pressure is also needed for the formation of $Li_5Ln_5Si_4N_{12}$ (Ln = La, Ce). Therefore, the combination of NaN_3 and elemental lithium as starting materials yielded the title compounds, corroborating the necessity of a nitrogen pressure inside the ampoule. The obtained products exhibit air and moisture sensitivity, similar to related chain type nitridosilicates, probably due to their low condensation degree.[13,14,16]

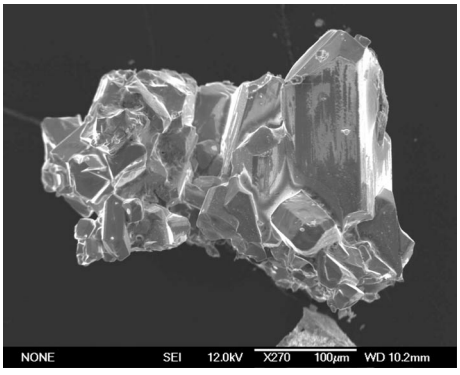

Figure 1. SEM image of $Li_5Ce_5Si_4N_{12}$.

Crystal Structure

X-ray structure analysis revealed two possible tetragonal space groups for the title compounds, namely *P*4/*nbm* (no. 125, centrosymmetric) and $P\bar{4}b2$ (no. 117, non-centrosymmetric). Solely the refinement in space group $P\bar{4}b2$ gave a reasonable structural model with satisfactory *R* values. The resulting flack parameters were indicative for inversion twinning, which was confirmed for both compounds. Details of the crystal structure determination are listed in Table 1. All atoms were refined anisotropically except for the Li positions.

Table 1. Crystallographic data of $Li_5Ln_5Si_4N_{12}$.

	$Li_5La_5Si_4N_{12}$	$Li_5Ce_5Si_4N_{12}$
Formula mass [g mol^{-1}]	1009.73	1015.78
Crystal system	tetragonal	
Space group	$P\bar{4}b2$ (no. 117)	
Cell parameters [pm]	a = 1142.8(16) c = 557.30(11)	a = 1097.78(16) c = 551.43(11)
Cell volume [10^6 pm^3]	V = 679.59(19)	V = 664.54(19)
Formula units/cell	2	
Crystal size [mm^3]	$0.09 \times 0.04 \times 0.01$	$0.08 \times 0.03 \times 0.01$
$\rho_{calcd.}$ [g cm^{-3}]	4.934	5.076
μ [mm^{-1}]	15.74	17.151
F(000)	880	890
Diffractometer	Stoe IPDS 1	
Temperature [K]	293(2)	293(2)
Radiation, monochromatic	Mo-K_α, (λ = 71.073 pm), graphite	
Absorption correction	multi scan	
θ range [°]	2.3–30.5	
Measured reflections	6002	6615
Independent reflections	782	973
Observed reflections	748	873
Refined parameters	56	56
Flack parameter	0.41(8)	0.47(5)
GoF	1.233	1.097
R indices [$F_o^2 \geq 2\sigma(F_o^2)$]	R_1 = 0.0482, $wR2$ = 0.1278	R_1 = 0.0294, $wR2$ = 0.0749
R indices (all data)	R_1 = 0.0498, $wR2$ = 0.1293[a]	R_1 = 0.0334, $wR2$ = 0.0760[b]
Max./min. residual electron density [e Å^{-3}]	2.22/–1.50	1.273/–2.385

[a] $w = 1/[\sigma^2(F_o^2) + (0.0932\ P)^2 + 0.00\ P]^{-1}$ where $P = (F_o^2 + 2\ F_c^2)/3$. [b] $w = 1/[\sigma^2(F_o^2) + (0.0473\ P)^2 + 0.00\ P]^{-1}$ where $P = (F_o^2 + 2\ F_c^2)/3$.

The majority of nitridosilicates described so far exhibit highly condensed network structures with a degree of condensation $\kappa \geq 1{:}2$ (i.e. molar ratio Si/N). Less condensed nitridosilicate anions with $\kappa < 1{:}2$ are only scarcely known. Recently, we reported on Eu_2SiN_3, which consists of nonbranched *zweier* chains – a structural feature that has been unknown for nitridosilicates so far. $Li_5Ln_5Si_4N_{12}$ with Ln = La, Ce contain nonbranched *zweier* chains of corner sharing SiN_4 tetrahedra (cf. Figure 2) analogously to

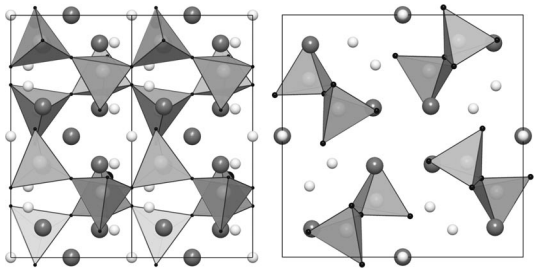

Figure 2. Crystal structure of $Li_5Ln_5Si_4N_{12}$ with Ln = La, Ce. Left: view along [100], Ln atoms dark gray, Li^+ white, SiN_4 tetrahedra gray. Right: view along [001], the tetrahedral tips of the chains are rotated clockwise by 90° relatively to each other.

Eu_2SiN_3 and is therefore another rare example for nitridosilicates with a low degree of condensation. The single chains run along [001] and the four chains within the unit cell are rotated along the *c*-axis by 90°. Moreover, the nitridosilicate chains feature a stretching factor f_S = 0.981 for $Li_5La_5Si_4N_{12}$, and f_S = 0.977 for $Li_5La_5Si_4N_{12}$, respectively.[24] These values resemble that of the mineral johannsenite ($CaMn[Si_2O_6]$; f_S = 0.98).[17] In contrast, the stretching factor in Eu_2SiN_3 reaches a maximum value of f_S = 1.0. Distances Si–N range between 170.9(7)–174.9(4) pm for the cerium and 174.0(10)–176.3(7) pm for the $Li_5La_5Si_4N_{12}$ and $Li_5Ce_5Si_4N_{12}$, respectively. The values are in the typical range of nitridosilicates.[25]

There are two crystallographically independent Ln-sites occupying Wyckoff positions 8*i* (Ln1) and 2*d* (Ln2). The Ln1 atoms are surrounded by seven nitrogen atoms building a mono-capped distorted octahedron. The Ln2 positions exhibit a distorted octahedral coordination geometry made up of nitrogen (cf. Figure 3, a). In the secondary coordination sphere Ln2 is coordinated by two Li2 atoms building alternating Ln–Li chains parallel to the *c*-axis. The interatomic distances for Ln1–N range between 249.9(9) to 292.3(9) pm and for Ln2–N between 251.6(9) and 270.6(11) pm [cf. Table 2; 247.8(8)–292.2(5) pm and 250.5(7)–270.4(9) pm for Ln = Ce, respectively]. These distances correspond well with other known lanthanum nitridosilicates (e.g. $La_3Si_6N_{11}$, $LaSi_3N_5$ or $La_5Si_3N_9$).[13,26] Analogously, the distances Ce–N are in the typical range of cerium containing nitridosilicates.[26]

Table 2. Selected interatomic distances [pm] for $Li_5Ln_5Si_4N_{12}$ (Ln = La, Ce). Standard deviations are given in parentheses.

		La	Ce
Ln1–N2		249.9(9)	247.8(8)
Ln1–N2		253.2(10)	249.3(8)
Ln1–N3		257.7(4)	255.2(4)
Ln1–N1		260.1(9)	259.0(7)
Ln1–N2		266.4(9)	260.8(5)
Ln1–N4		266.9(5)	265.3(4)
Ln1–N2		292.3(9)	292.2(5)
Ln2–N1	(4x)	251.6(9)	250.5(7)
Ln2–N4	(2x)	270.6(11)	270.4(9)
Ln2–Li2	(2x)	278.7(2)	275.7(2)
Li1–N1		207(3)	205(2)
Li1–N2		210(3)	218(2)
Li1–N1		221(3)	215(2)
Li1–N3		225(3)	226(2)
Li2–N1	(4x)	221.7(10)	218.5(7)
Li1–Li2		281(3)	271(2)
Li1–Li1		225(6)	216(4)

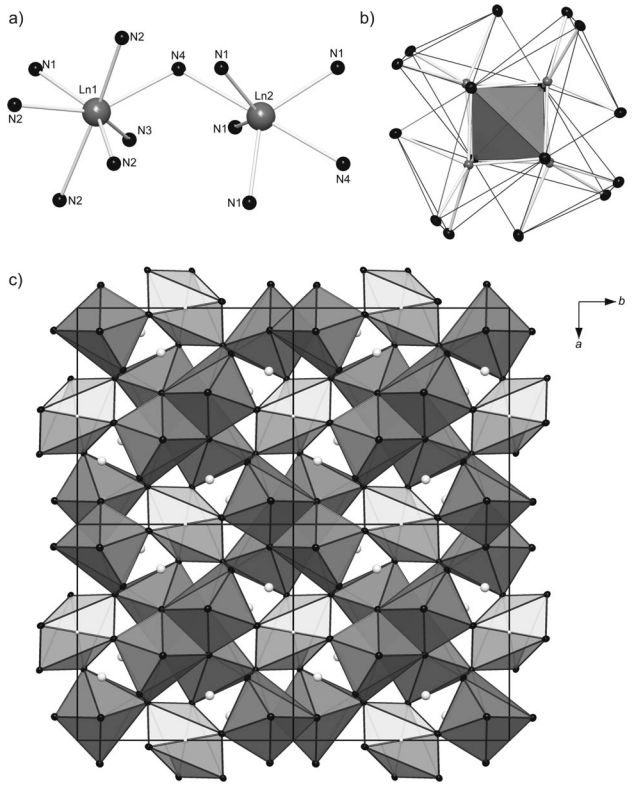

Figure 3. a) Coordination of Ln in $Li_5Ln_5Si_4N_{12}$ (Ln = La, Ce); b) tetrahedral vacancy built up by four LnN_7 polyhedra; c) depiction of the Ln–N polyhedra; dark gray LnN_7 polyhedra, light gray LnN_6 polyhedra. Li^+ positions are depicted in white, Si atoms omitted for clearity.

The Ln1 polyhedra are connected via common edges and corners, forming groups of four polyhedra, building up strands along [001]. Within these strands the polyhedra enclose nearly regular tetrahedral voids (cf. Figure 3, b). The latter ones exhibit a distance of 210.3(2) pm between their centers and the surrounding N atoms. However, no residual electron density could be found within these voids. Moreover, occupying the voids with Li would lead to a charge within the compound, which cannot be counterbalanced by nitrogen. The LnN_7 strands are connected to each other via common corners and LnN_6 octahedra, which are depicted in light gray (cf. Figure 3, c).

The two crystallographically independent Li^+ sites are coordinated by nitrogen atoms in a distorted tetrahedral fashion, forming $[Li_5N_{10}]^{25-}$ building units. The distances Li–N vary between 210(3) and 221.7(10) pm for Ln = La, and 215(2)–225.6(19) pm for Ln = Ce, respectively (cf. Table 2). These distances are in good accordance with previously reported lithium containing nitridosilicates.[27,28] In the second coordination sphere five Li^+ ions form a "bow-tie" arrangement (cf. Figure 4, left). Hereby, the Li2 positions are surrounded by Li1 atoms in a tetrahedrally distorted way. Interestingly, the Li1–Li1 distances are quite short [Li1–Li1: 225(6) pm for $Li_5La_5Si_4N_{12}$, 216(4) pm for $Li_5Ce_5Si_4N_{12}$]. However, the values exceed the range of the sum of the ionic radii.[29,30] Comparable distances Li–Li have been observed in other lithium nitridosilicates and lithium nitridophosphates [e.g. $Li_2Sr_4Si_4N_8O$: 199(3) pm; Li_7PN_4: 224.9 pm].[23,31] The planes spanned by Li1–Li1–Li2 enclose almost a right angle δ = 94.9(2)° for Ln = La, δ = 92.1(2)° for Ln = Ce (cf. Figure 4, right).

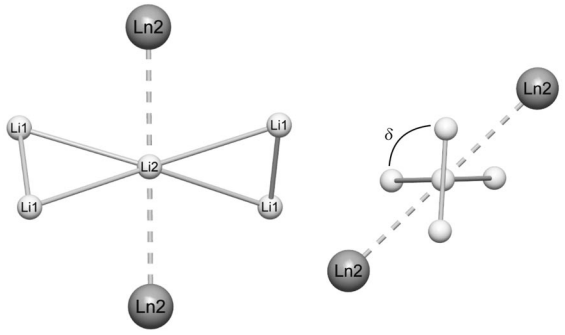

Figure 4. Lithium arrangement with coordinated Ln2. Right: depiction of the angle δ spanned up by the two Li1–Li1–Li2 planes.

Solid-State MAS NMR

The ^{7}Li solid-state MAS NMR spectrum of $Li_5La_5Si_4N_{12}$ shows one isotropic intense peak at 1.6 ppm with a full width at half maximum (FWHM) of 3.5 ppm (Figure 5). This chemical shift is in good accordance with other lithium-containing nitridosilicates (e.g. Li_2SiN_2 δ = 1.7 ppm,[27] $LiSi_2N_3$, δ = 1.3 ppm,[28] $Li_4Ca_3Si_2N_6$ δ = 2.0 ppm).[23] Due to the low resolution of ^{7}Li solid-state MAS NMR no differentiation of the two crystallographically independent lithium sites can be observed in the spectrum. This is in accordance with other lithium nitridosilicates, e.g. Li_2SiN_2 exhibits eight crystallographically independent lithium sites, whereas only one sharp signal in the NMR spectrum can be found.[27]

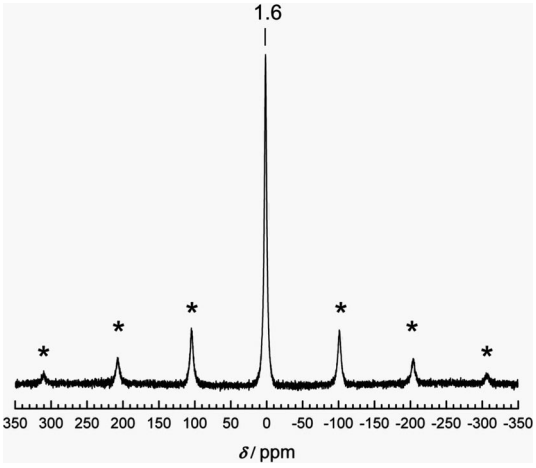

Figure 5. Solid-state MAS NMR of $Li_5La_5Si_4N_{12}$ of ^{7}Li. Rotation bands are indicated by asterisks (rotation frequency 20 kHz).

Lattice Energy Calculations According to the Maple Concept

Lattice energy calculations (MAPLE: Madelung part of lattice energy)[29,32–34] were performed to corroborate the crystal structures of $Li_5Ln_5Si_4N_{12}$ with Ln = La, Ce. Hereby, exclusively electrostatic interactions in an ionic crystal were considered, depending on the charge, distance and the coordination spheres of the constituting atoms. The total MAPLE values for the two title compounds correspond well with the sum of the total MAPLE values of the constituting binary nitrides (cf. Table 3). Furthermore, the calculated partial MAPLE values of the crystallographically different atoms are in good agreement with the atom type ranges from comparable compounds in the literature.[35,36]

Table 3. Results of the MAPLE calculations [kJ/mol] for $Li_5Ln_5Si_4N_{12}$ (Ln = La, Ce); Δ = difference.[a]

	La	Ce
Ln^{3+}	4061; 3734	4079; 3884
Si^{4+}	9896	9988
$N^{[1]3-}$	4823; 4768	4850; 4842
$N^{[2]3-}$	5355; 5586	5451; 5586
Li^+ (8*i*)	700	727
Li^+ (2*b*)	784	775
Total MAPLE	123619	124800
Δ	0.75%	0.16%

Total MAPLE (5/3 Li_3N + 5 LaN + 4/3 Si_3N_4): 122698 kJ/mol
Total MAPLE (5/3 Li_3N + 5 CeN + 4/3 Si_3N_4): 124997 kJ/mol

[a] Typical partial MAPLE values [kJ/mol]: La^{3+}: 3500–5000; Ce^{3+}: 3800–4800; Si^{4+}: 9000–10200; $N^{[1]3-}$: 4300–5000; $N^{[2]3-}$: 4600–6000; Li^+: 600–860.[35,36]

MAPLE calculations with a theoretically occupied tetrahedral void (built up by LnN_7 polyhedra, cf. Figure 3, b) were performed. However, the partial values for these hypothetical Li sites shift to anomalous MAPLE values, corroborating that the tetrahedral void are not occupied in accordance with the crystal structure determination.

Conclusions

In this contribution, employment of lithium melts for the synthesis of lithium nitridosilicates could be expanded to compounds containing rare earth elements. Despite the higher melting points of the rare-earth metals compared to alkaline earth elements, rather low reaction temperatures of 900 °C can be applied. Two new less condensed lithium rare-earth nitridosilicates, namely $Li_5Ln_5Si_4N_{12}$ (Ln = La, Ce) have been synthesized, comprising the structural motif of nonbranched *zweier* chains – a structural feature for nitridosilicates hitherto only known for Eu_2SiN_3. Thus, the lithium flux method seems to be a promising approach for further extension to the synthesis of nitridosilicates of the late rare earth elements and gives access to compounds with a high metal content.

Experimental Section

Synthesis: All manipulations were performed with rigorous exclusion of oxygen and moisture in flame-dried Schlenk-type glassware on a Schlenk line interfaced to a vacuum line (10^{-3} mbar) or in an argon-filled glove box (Unilab, MBraun, Garching, O_2 < 0.1 ppm, H_2O < 0.1 ppm). Argon (Messer-Griessheim, 5.0) was purified by passage through columns of silica gel (Merck), molecular sieves (Fluka, 4 Å), KOH (Merck, ≥85%), P_4O_{10} (Roth, ≥99%, granulate) and titanium sponge (Johnson Matthey, 99.5%, grain size ≤ 0.8 cm) at 700 °C. For the syntheses of the title com-

pounds tantalum tubes (wall thickness 0.5 mm, internal diameter 10 mm, length 300 mm) were cleaned and their oxide layer removed by treating with a mixture of HNO_3 (concd.) and HF (40%). The tubes were weld shut in an arc furnace under 1 bar purified argon. During this procedure, the crucible holder was water cooled in order to avoid chemical reactions during welding.

Synthesis of $Li_5La_5Si_4N_{12}$: For the synthesis of $Li_5La_5Si_4N_{12}$ silicon diimide (50 mg, 0.86 mmol; synthesized according to literature[37]), $LaCl_3$ (216 mg, 0.88 mmol) and NaN_3 (18.8 mg, 0.29 mmol, Acros, 99%) were mixed in an agate mortar, filled in a tantalum tube and covered with lithium (40 mg, 5.73 mmol, Alfa Aesar, 99.9%) in a glove box. The sealed tantalum ampoule was placed into a silica tube under argon, which was placed in the middle of a tube furnace. The temperature was raised to 900 °C (rate 2 °C min^{-1}), maintained for 24 h and cooled down to 500 °C (rate 0.09 °C min^{-1}). Subsequently, the sample was quenched down to room temperature by switching off the furnace. The sample contained $Li_5La_5Si_4N_{12}$ as brownish, air- and moisture-sensitive crystals.

Synthesis of $Li_5Ce_5Si_4N_{12}$: $Li_5Ce_5Si_4N_{12}$ can be synthesized with an analogous approach, however, crystals of better quality can be obtained as follows. $Li_5Ce_5Si_4N_{12}$ was synthesized starting from silicon diimide[37] (23.3 mg, 0.39 mmol), $CeCl_3$ (74 mg, 0.30 mmol, Alfa Aesar, 99.99%) and LiN_3 (14 mg, 0.30 mmol). The starting materials were mixed in an agate mortar, filled in a tantalum tube and covered with lithium (14 mg, 20 mmol). The tantalum ampoule was placed in a silica tube under argon and heated to 900 °C (rate 5 °C min^{-1}). The temperature was kept for 12 h, subsequently, the tube was cooled down to 500 °C (rate 0.2 °C min^{-1}) and quenched to room temperature by switching off the furnace. The sample contained $Li_5Ce_5Si_4N_{12}$ as dark reddish, air- and moisture-sensitive crystals.

Chemical Analyses: Scanning electron microscopy was performed on a JEOL JSM-6500F equipped with a eld emission gun at an acceleration voltage of 10 kV with a Si/Li EDX detector (Oxford Instruments, model 7418). Samples were prepared by placing single crystals on adhesive conductive pads and subsequently coating them with a thin conductive carbon film. Each EDX spectrum (Oxford Instruments) was recorded with the analyzed area limited onto one single crystal to avoid the influence of possible contaminating phases. Analysis of three spots per crystallite showed average atomic ratio Ln/Si = 5:4 (Ln = La, Ce) which corroborates the formation of $Li_5Ln_5Si_4N_{12}$ (Ln = La, Ce). The determined compositions are in accordance to the structure model within the typical error ranges with regard to the fact that lithium cannot be detected by this method [calcd. (atom-%). Ln 19, Si 15, N 46; found (atom-%) La 20, Si 20, N 70; Ce 20, Si 11, N 62 O 2].

Single Crystal X-ray Analysis: Single crystals of $Li_5Ln_5Si_4N_{12}$ with Ln = La, Ce were isolated under a microscope, which is integrated in a glove box, enclosed in glass capillaries (Ø = 0.2 mm), and sealed under argon. Single-crystal X-ray diffraction data were collected at room temperature on a STOE IPDS I diffractometer (Stoe and Cie GmbH, Darmstadt) with Mo-K_α radiation (λ = 0.71073 Å, graphite monochromator). The structures were solved by direct methods after semi-empirical absorption correction. For the structure solution and refinement the program package SHELX97 was used.[38]

Further details on the crystal structure investigations may be obtained from the Fachinformationszentrum Karlsruhe, 76344 Eggenstein-Leopoldshafen, Germany (Fax: +49-7247-808-666; E-mail: crysdata@fiz-karlsruhe.de), on quoting the depository number CSD-421528 (Ln = La) and -421527 (Ln = Ce).

X-ray Powder Diffraction: X-ray powder diffraction data were collected on a STOE STADI P diffractometer with Ge(111)-monochromatized Mo-$K_{\alpha1}$ radiation (λ = 0.71073 Å) in Debye–Scherrer geometry. The samples were enclosed in silica tubes and sealed under argon.

Solid-State MAS NMR: Solid-state NMR experiments were performed on a Bruker Advance DSX 500 spectrometer with an external field of 11.75 T for $Li_5La_5Si_4N_{12}$. The ^7Li spectrum was recorded with direct excitation using a commercial 2.5 mm triple-resonance MAS probe at the frequency 194.415 MHz. All experiments were carried out at room temperature in ZrO_2 rotors. The chemical shifts of ^7Li are reported using the frequency ratios published by IUPAC [δ scale relative to 1% tetramethylsilane (TMS) in $CDCl_3$]. The one-dimensional ^7Li NMR spectrum was acquired with a 90° pulse length of 3.0 µs, a recycle delay of 32 s and at a sample spinning frequency of 20 kHz.

Supporting Information (see also the footnote on the first page of this article): PXRD patterns of $Li_5Ln_5Si_4N_{12}$ with Ln = La, Ce in comparison to the simulations from single-crystal structure analysis.

Acknowledgments

Tue authors are indebted to the following people for conducting the physical measurements: Thomas Miller and Dr. Oliver Oeckler (single-crystal X-ray diffractometry), Dr. Jörn Schmedt auf der Günne and Christian Minke (solid-state NMR); all from the Department Chemie, University of München (LMU). The authors gratefully acknowledge financial support from the Fonds der Chemischen Industrie (FCI) and the Deutsche Forschungsgemeinschaft (DFG), project SCHN 377/14-1. The authors acknowledge gratefully grants for S. L., M. Z. and S. P. by the Dr. Klaus Römer Foundation, Munich.

[1] W. Schnick, *Angew. Chem.* **1993**, *105*, 846–858; *Angew. Chem. Int. Ed. Engl.* **1993**, *33*, 806–818.
[2] R.-J. Xie, N. Hirosaki, *Sci. Technol. Adv. Mater.* **2007**, *8*, 588–600.
[3] Y. Q. Li, G. deWith, H. T. Hintzen, *J. Solid State Chem.* **2008**, *181*, 515–524.
[4] R.-J. Xie, N. Hirosaki, N. Kimura, K. Sakuma, M. Mitomo, *Appl. Phys. Lett.* **2007**, *90*, 191101/1–191101/3.
[5] X. Piao, T. Horikawa, H. Hanzawa, K. Machida, *Appl. Phys. Lett.* **2006**, *88*, 161908/1–161908/3.
[6] R. Mueller-Mach, G. Mueller, M. R. Krames, H. A. Höppe, F. Stadler, W. Schnick, T. Juestel, P. Schmidt, *Phys. Status Solidi A* **2005**, *202*, 1727–1732.
[7] H. Huppertz, W. Schnick, *Angew. Chem.* **1996**, *108*, 2115–2116; *Angew. Chem. Int. Ed. Engl.* **1996**, *35*, 1983–1984.
[8] C. Schmolke, S. Lupart, W. Schnick, *Solid State Sci.* **2009**, *11*, 305–309.
[9] H. Huppertz, W. Schnick, *Chem. Eur. J.* **1997**, *3*, 249–252.
[10] M. Yamada, T. Naitou, K. Izuno, H. Tamaki, Y. Murazaki, M. Kameshima, T. Mukai, *Jpn. J. Appl. Phys.* **2003**, *42*, L20–L23.
[11] H. A. Höppe, H. Lutz, P. Morys, W. Schnick, A. Seilmeier, *J. Phys. Chem. Solids* **2000**, *61*, 2001–2006.
[12] W. Schnick, H. Huppertz, R. Lauterbach, *J. Mater. Chem.* **1999**, *9*, 289–296.
[13] C. Schmolke, D. Bichler, D. Johrendt, W. Schnick, *Solid State Sci.* **2008**, *10*, 389–394.
[14] S. Lupart, W. Schnick, *Acta Crystallogr., Sect. E* **2009**, *65*, i43.
[15] Q^1-type SiN_4 tetrahedra are connected with one vertex to the next tetrahedron, therefore representing a terminal unit.

[16] M. Zeuner, S. Pagano, P. Matthes, D. Bichler, D. Johrendt, T. Harmening, R. Pöttgen, W. Schnick, *J. Am. Chem. Soc.* **2009**, *131*, 11242–11248.
[17] F. Liebau, *Structural chemistry of Silicates*, Springer, Berlin, **1985**, p. 80 ff.
[18] H. Yamane, F. J. DiSalvo, *J. Alloys Compd.* **1996**, *240*, 33–36.
[19] Z. A. Gál, P. M. Mallinson, H. J. Orchard, S. J. Clarke, *Inorg. Chem.* **2004**, *43*, 3998–4006.
[20] R. J. Pulham, P. Hubberstey, *J. Nucl. Mater.* **1983**, *115*, 239–250.
[21] A. T. Dadd, P. Hubberstey, *J. Chem. Soc., Dalton Trans.* **1982**, 2175–2179.
[22] P. Hubberstey, P. G. Roberts, *J. Chem. Soc., Dalton Trans.* **1994**, 667–673.
[23] S. Pagano, S. Lupart, M. Zeuner, W. Schnick, *Angew. Chem.* **2009**, *121*, 6453–6456; *Angew. Chem. Int. Ed.* **2009**, *48*, 6335–6338.
[24] The stretching factor is defined by Liebau as $f_S = I_{chain}/(l_T \times P)$, with I_{chain}: the distance of one period; l_T: edge length of the tetrahedral; P: periodicity of the chain.
[25] F. Stadler, O. Oeckler, J. Senker, H. A. Höppe, P. Kroll, W. Schnick, *Angew. Chem.* **2005**, *117*, 573–576; *Angew. Chem. Int. Ed.* **2005**, *44*, 567–570.
[26] M. Woike, W. Jeitschko, *Inorg. Chem.* **1995**, *34*, 5105–5108.
[27] S. Pagano, M. Zeuner, S. Hug, W. Schnick, *Eur. J. Inorg. Chem.* **2009**, 1579–1584.
[28] M. Orth, W. Schnick, *Z. Anorg. Allg. Chem.* **1999**, *625*, 142631428.
[29] R. D. Shannon, *Acta Crystallogr., Sect. A: Cryst. Found. Crystallogr.* **1976**, *32*, 751–767.
[30] W. H. Baur, *Crystallogr. Rev.* **1987**, *1*, 59–83.
[31] W. Schnick, J. Lücke, *J. Solid State Chem.* **1990**, *87*, 101–106.
[32] R. Hübenthal, *Programm zur Berechnung des Madelunganteils der Gitterenergie*, version 4, University of Gießen, Germany, **1993**.
[33] R. Hoppe, *Angew. Chem. Int. Ed. Engl.* **1966**, *78*, 52–63; *Angew. Chem.* **1966**, *5*, 95–106.
[34] R. Hoppe, *Angew. Chem. Int. Ed. Engl.* **1970**, *82*, 7–16; *Angew. Chem.* **1970**, *9*, 25–34.
[35] H. A. Höppe, *Doctoral* Thesis, University of Munich, **2003**.
[36] K. Köllisch, *Doctoral* Thesis, University of Munich, **2001**.
[37] H. Lange, G. Wötting, G. Winter, *Angew. Chem. Int. Ed. Engl.* **1991**, *103*, 1606–1625; *Angew. Chem.* **1991**, *30*, 1579–1597.
[38] G. M. Sheldrick, *Acta Crystallogr., Sect. A* **2008**, *64*, 112.

Received: March 1, 2010
Published Online: May 14, 2010

